JOURNAL OF VIROLOGY, Aug. 2002, p. 7485–7494 Vol. 76, No. 15
0022-538X/02/$04.00+0 DOI: 10.1128/JVI.76.15.7485–7494.2002

Sequence Requirements for Viral RNA Replication and VPg Uridylylation Directed by the Internal *cis*-Acting Replication Element (*cre*) of Human Rhinovirus Type 14

Yan Yang,[1] Rene Rijnbrand,[1] Kevin L. McKnight,[1]† Eckard Wimmer,[2] Aniko Paul,[2] Annette Martin,[1,3] and Stanley M. Lemon[1]*

Department of Microbiology and Immunology, The University of Texas Medical Branch, Galveston, Texas 77555-1019[1]; Department of Molecular Genetics and Microbiology, State University of New York at Stony Brook, Stony Brook, New York 11794[2]; and Unité de Génétique Moléculaire des Virus Respiratoires, Institut Pasteur, 75724 Paris Cedex 15, France[3]

Received 24 January 2002/Accepted 30 April 2002

Until recently, the *cis*-acting signals required for replication of picornaviral RNAs were believed to be restricted to the 5′ and 3′ noncoding regions of the genome. However, an RNA stem-loop in the VP1-coding sequence of human rhinovirus type 14 (HRV-14) is essential for viral minus-strand RNA synthesis (K. L. McKnight and S. M. Lemon, RNA 4:1569-1584, 1998). The nucleotide sequence of the apical loop of this internal *cis*-acting replication element (*cre*) was critical for RNA synthesis, while secondary RNA structure, but not primary sequence, was shown to be important within the duplex stem. Similar *cre*s have since been identified in other picornaviral genomes. These RNA segments appear to serve as template for the uridylylation of the genome-linked protein, VPg, providing the VPg-pUpU primer required for viral RNA transcription (A. V. Paul et al., J. Virol. 74:10359-10370, 2000). Here, we show that the minimal functional HRV-14 *cre* resides within a 33-nucleotide (nt) RNA segment that is predicted to form a simple stem-loop with a 14-nt loop sequence. An extensive mutational analysis involving every possible base substitution at each position within the loop segment defined the sequence that is required within this loop for efficient replication of subgenomic HRV-14 replicon RNAs. These results indicate that three consecutive adenosine residues (nt 2367 to 2369) within the 5′ half of this loop are critically important for *cre* function and suggest that a common RNNNAA RNNNNNNR loop motif exists among the *cre* sequences of enteroviruses and rhinoviruses. We found a direct, positive correlation between the capacity of mutated *cre*s to support RNA replication and their ability to function as template in an in vitro VPg uridylylation reaction, suggesting that these functions are intimately linked. These data thus define more precisely the sequence and structural requirements of the HRV-14 *cre* and provide additional support for a model in which the role of the *cre* in RNA replication is to act as template for VPg uridylylation.

The family *Picornaviridae* is one of the largest groups of nonenveloped, single-stranded, positive-sense RNA viruses. It comprises nine distinct genera, of which five (the enteroviruses, rhinoviruses, aphthoviruses, cardioviruses, and hepatoviruses) are important human and animal pathogens (23). These genera are distinguished from each other by differences in the proteins they express, but the RNA genomes of each have a similar organization, with a lengthy 5′ nontranslated region (5′ NTR) followed by a single, large open reading frame encoding a single polyprotein, a 3′ NTR, and a genetically templated 3′-terminal poly(A) tail (28). Since it is positive sense, the virion RNA acts directly as message, programming the translation of the polyprotein following its release into the cytoplasm. Virion RNA and synthetic genome-length RNA derived from recombinant cDNA clones are thus infectious when transfected into permissive cells, giving rise to virus particles and subsequent rounds of virus replication (22).

An unusual feature of the genomic RNA of picornaviruses is that it lacks the 5′-terminal cap structure present in most eucaryotic mRNAs and is instead covalently linked to a small, virally encoded protein, VPg (3, 8). An internal ribosomal entry site located within the 5′ NTR directs the cap-independent translation of the polyprotein (6, 19), so that the cellular translational machinery thus bypasses the 5′ end of the genome. The polyprotein contains three major functional segments, defined in part by the order of cleavage events that occur during its processing by one or more viral proteases (26). In the case of the enteroviruses and rhinoviruses, the most N-terminal segment, P1, contains four capsid proteins, VP4, VP2, VP3, and VP1, while the P2 and P3 segments are comprised of nonstructural proteins involved in protein maturation and RNA replication. These include $2A^{pro}$, 2B, 2C, 3A, 3B (VPg), $3C^{pro}$, and $3D^{pol}$ and their functional precursors, 2BC, 3AB, and $3CD^{pro}$ (15).

In broad outline, the replication of picornaviral RNAs follows a two-step process. Upon entry into host cells and un-

* Corresponding author. Mailing address: Department of Microbiology & Immunology, The University of Texas Medical Branch, Galveston, TX 77755-1019. Phone: (409) 772-4793. Fax: (409) 772-9598. E-mail: smlemon@utmb.edu.

† Present address: Eli Lilly and Company, Indianapolis, IN 46285.

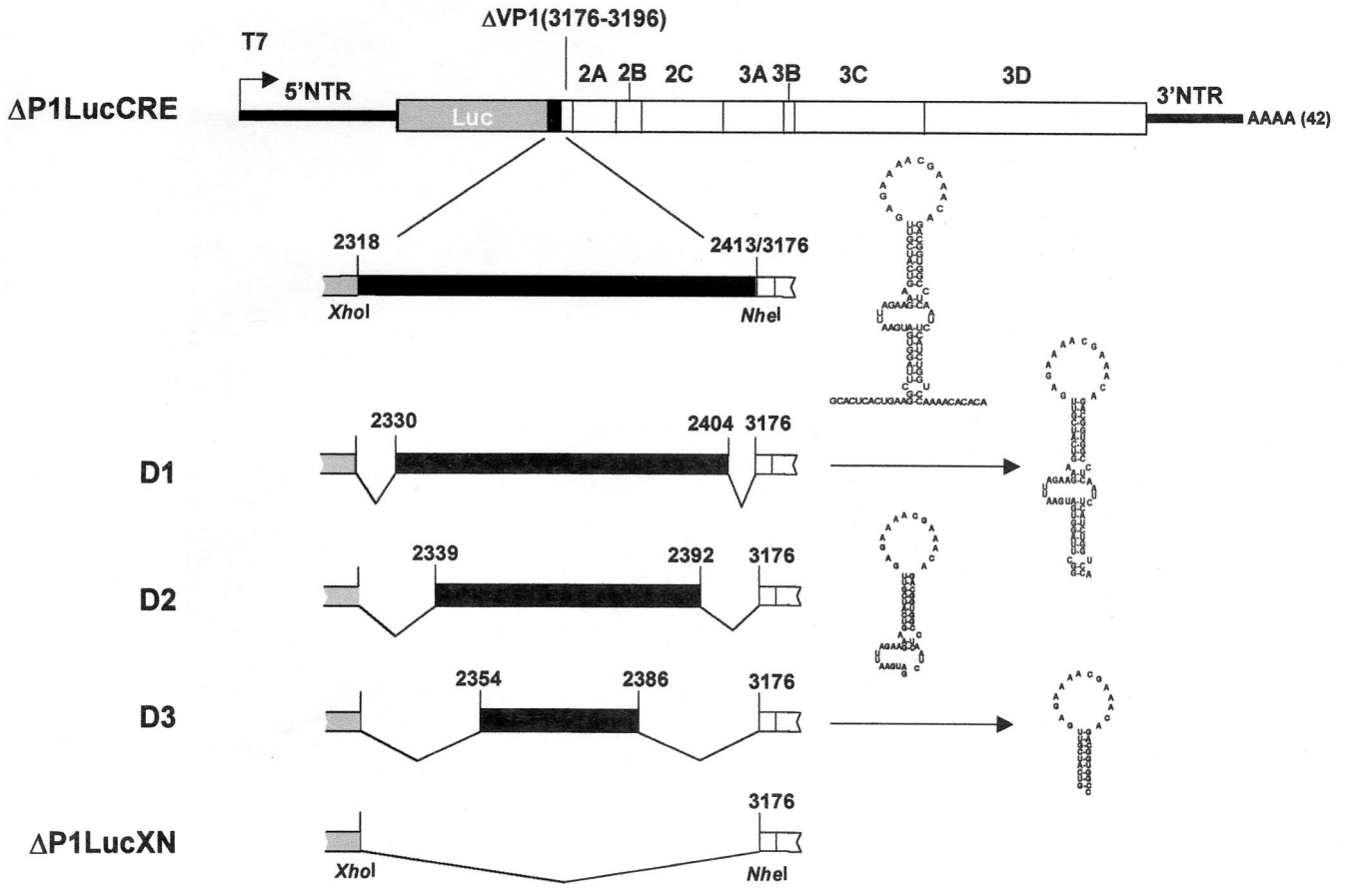

FIG. 1. Organization of the subgenomic HRV-14 replicon, ΔP1LucCRE. In ΔP1LucCRE, all of the P1 region was replaced with luciferase coding sequence, except for the 21 nt coding for the carboxy-terminal 7 aa of VP1 (12). The HRV-14 *cre* was inserted in frame between the luciferase and residual VP1 coding sequences at two engineered restriction sites, *Xho*I and *Nhe*I. D1, D2, and D3 deletion mutants contain progressively lengthier deletion mutations flanking the apical stem-loop of the HRV-14 *cre* and were constructed as described in Materials and Methods. The MFOLD-predicted secondary structures of the *cre* in the parental HRV-14 *cre* and the three deletion mutants are shown to the right of each construct. ΔP1LucXN is identical to ΔP1LucCRE, but lacks any *cre* sequence and is replication incompetent when transfected into HeLa cells (12).

coating of the virus, the incoming positive-strand genome is transcribed into complementary minus-strand RNA by a replicase complex, the catalytic unit of which, $3D^{pol}$, uses a uridylylated form of VPg (VPg-pUpU) as a primer (18). This minus-strand RNA then serves as a template for the production of new, plus-strand, progeny genomes. Although the basic steps of replication are well known, relatively little is understood about the details of these processes. One of the important, yet incompletely answered questions is how the viral replicase specifically selects only viral RNA species for amplification in these reactions, because the 3′-terminal poly(A) sequence of the genomic RNA is indistinguishable from the 3′ termini of cellular mRNAs.

Until recently, it was generally believed that the 5′ and 3′ NTRs of picornaviral RNA contain the *cis*-acting signals necessary for the initiation of viral RNA replication (28). The specificity of genome amplification was thought to result from interactions of the replicase complex with unique *cis*-acting signals located in the 5′ and 3′ NTRs (1, 13, 14, 21, 22, 25, 27). However, McKnight and Lemon (11, 12) demonstrated that an internal *cis*-acting replication element (*cre*) was necessary for the initiation of RNA synthesis during replication of human rhinovirus type 14 (HRV-14). Although this replication element is located in the long open reading frame, within the segment encoding the VP1 capsid protein, the role of the *cre* in replication is dependent upon its RNA structure and not its protein-coding capacity (12). Mutational analysis and computer folding algorithms suggested that the *cre* forms a complex stem-loop structure within the positive-strand RNA that is required for initiation of minus-strand RNA synthesis (Fig. 1) (12).

Following the identification of the HRV-14 *cre*, similar internal replication signals were identified within the open reading frames of Theiler's virus, a cardiovirus (9), poliovirus type 1 (PV-1) (5), and, more recently, HRV-2 (4). The latter observations suggest that an internally located *cre* may be a common feature of the RNA replication schemes of all picornaviruses. The RNA segments comprising these putative *cre*s can be folded into relatively simple stem-loop structures, but the elements differ in terms of their primary nucleotide sequence

as well as their location within the open reading frame. In cardioviruses, the *cre* is located in the VP2 region (9). In contrast, the PV-1 *cre* is not located in the P1 capsid region, but in the 2C (P2) region (5), while the HRV-2 *cre* is located within the 2A coding sequence (4). Studies by Paul et al. (17) indicate that the *cre* acts as the primary template for uridylylation of VPg by the $3D^{pol}$ polymerase in vitro. In addition, a recent mutational analysis of the poliovirus polymerase indicates that amino acid residues on the surface of the protein that are essential for uridylylation of VPg are also involved in the interaction of the polymerase with the membrane-bound 3AB precursor protein (10). Taken together, these data suggest that the *cre* plays a critical role in bringing viral RNA into the replication complex and in initiating VPg uridylylation, the first step in the process of viral RNA replication.

Here, we describe experiments aimed at better defining both the sequence and structural requirements for *cre* function during the replication of HRV-14 RNA. We show that the fully functional *cre* resides within a 33-nucleotide (nt) RNA segment that is predicted to form a simple stem-loop structure. By introducing single-base substitutions at each position within the loop sequence, we have determined which nucleotides are essential for replication and which nucleotide substitutions are tolerated without significant degradation of *cre* function. We further show that the ability of individual mutant *cre* sequences to support RNA replication is closely correlated with their ability to serve as template for the uridylylation of VPg in an in vitro reaction.

MATERIALS AND METHODS

Cells. HeLa cells were obtained from the American Type Culture Collection and maintained in Dulbecco's modified Eagle's medium (DMEM; Gibco/BRL) with 5% fetal bovine serum (FBS).

HRV-14 RNA replication assay. The replication of HRV-14 RNA was monitored by measurement of luciferase expression in HeLa cells transfected with ΔP1LucCRE RNA (12). ΔP1LucCRE is a subgenomic RNA replicon in which most of the P1 segment of the HRV-14 genome has been replaced by an in-frame insertion of the firefly luciferase coding sequence (Fig. 1). Replicon transcripts were obtained by T7 polymerase-mediated transcription (T7 MEGAscript; Ambion) of pΔP1LucCRE and related plasmids after linearization at the unique *Mlu*I site downstream of the poly(A) tail. The integrity and abundance of transcript RNAs were determined by agarose gel analysis. These transcripts were electroporated into HeLa cells as previously described (12). Briefly, 5×10^6 cells were electroporated with 20 μg of RNA by using a GenePulser II electroporation apparatus (Bio-Rad) with the pulse controller unit set at 980 V and 25 μF and with maximum resistance. The cells were subsequently seeded into a six-well plate and cultured in DMEM with 5% FBS at 34°C until processed for luciferase assays. Luciferase activity was measured in cell lysates with the Promega luciferase assay kit. Briefly, 125 μl of lysis buffer (Promega) was added to each well of a six-well plate, and the lysate was stored at −70°C until assay. Luciferase quantitation was carried out as described by the supplier with a TD-20/20 luminometer (Turner Designs).

Site-directed mutagenesis of the *cre* loop segment. Site-directed mutagenesis was facilitated by subcloning a DNA fragment containing the *cre* sequence from the plasmid pΔP1LucCRE (12) into the vector pLITMUS 29 (New England Biolabs) at *Xho*I and *Nco*I restriction endonuclease sites. Mutations were introduced with the QuickChange site-directed mutagenesis kit (Stratagene) with a series of degenerate oligonucleotide primers containing a variety of single-base substitutions within the region representing the *cre* loop segment. The products of these mutagenesis reactions were characterized by DNA sequencing. Selected mutants were digested with *Xho*I and *Nhe*I, and a small DNA fragment was inserted into pΔP1LucCRE at the *Xho*I and *Nhe*I sites flanking the *cre* region (Fig. 1). All substitutions were confirmed by DNA sequencing.

Construction of *cre* mutants with in-frame deletions. To define the minimal functional *cre* sequence, PCR mutagenesis was used to create in-frame deletions upstream and downstream of the previously defined apical stem-loop of the *cre*, as shown in Fig. 1. The oligonucleotide primers for PCRs leading to the construction of the deletion mutant D1 were D1+ (CCGCTCGAGGGCTTAGGT GATG) and D1− (CTAGCTAGCTGGACCAGATGAGATTG); for mutant D2, the primers were D2+ (CCGCTCGAGGATGAATTAGAAGAAG) and D2− (CTAGCTAGCGATTGAGGCCACCG); and for mutant D3, the primers were D3+ (CCGCTCGAGGTCATCGTTGAG) and D3− (CTAGCTAGCGG CCACCGTCTGTTTCG). The resulting PCR products were digested with *Xho*I and *Nhe*I and ligated into pΔP1LucCRE as described above. All regions subjected to PCR amplification were sequenced to verify the deletions and ensure that no undesired mutations were introduced.

Computer-based prediction of RNA structures. RNA secondary structure was predicted by using the MFOLD program with the Zuker energy minimization algorithm (Genetics Computer Group, University of Wisconsin).

In vitro VPg uridylylation assay. Wild-type and mutant HRV-14 *cre* templates (representing HRV14 nt 2318 to 2413) were prepared by T7 transcription of DNA fragments amplified from the cognate plasmid DNAs by PCR with the oligonucleotide primers E-T7-5′CRE (CCGGAATTCTAATACGACTCACTA TAGGGGCACTCACTGAAGGC) and N-3′CRE (CTAGCTAGCTGTGTGT TTTG). Transcription reactions were carried out with the T7 Megashortscript kit (Ambion), and transcript RNAs were purified by phenol-chloroform extraction and ethanol precipitation prior to use in the uridylylation reactions.

The uridylylation of a synthetic PV-1 VPg oligopepetide with wild-type and mutant HRV-14 *cre* RNA templates was assayed as previously described (17). Briefly, reaction mixtures (20 μl) containing 50 mM HEPES buffer (pH 7.5), 8% glycerol, 3.5 mM magnesium acetate, 0.5 μg of HRV-14 *cre* transcript RNA, 2 μg of synthetic PV-1 VPg, 1 μg of purified PV-1 3D polymerase, 0.75 μCi of [α-^{32}P]UTP (3,000 Ci/mmol; Dupont-NEN), 10 μM unlabeled UTP, and 0.5 μg of PV-1 $3CD^{pro}$[$3C^{pro}$(H40A)] were incubated at 34°C for 60 min. Reaction products were analyzed by Tricine-sodium dodecyl sulfate-polyacrylamide gel electrophoresis (SDS-PAGE) (Bio-Rad) with 13.5% polyacrylamide. Gels were dried and subjected to autoradiography. Reaction products were quantitated by PhosphorImager (Molecular Dynamics) analysis.

RESULTS

RNA structure requirement for HRV-14 *cre* function. To analyze the effects of nucleotide deletions and substitutions within the previously identified 96-nt HRV-14 *cre* segment (Fig. 1), we utilized a replication-competent, subgenomic RNA replicon, ΔP1LucCRE (Fig. 1). This replicon was constructed from an HRV-14 infectious clone (7, 12) by replacing the P1, capsid protein-coding segment of the genome with the firefly luciferase coding sequence. Retention of the 21-nt sequence encoding the carboxy-terminal 7 amino acids of VP1 allowed for recognition and processing of the polyprotein at the VP1/$2A^{pro}$ cleavage site by the $2A^{pro}$ proteinase. The 96-nt *cre* sequence (nt 2318 to 2413) was inserted in frame at unique restriction sites engineered between the 3′ end of the luciferase sequence and the residual VP1 sequence (12) (Fig. 1).

Replication of the subgenomic RNA transcribed from this plasmid was monitored by measuring luciferase expression following transfection of the RNA into cultured HeLa cells. As shown in Fig. 2A, transfection of ΔP1LucCRE RNA gave rise to an increase in luciferase activity between 3 and 24 h. In contrast, transfection of a similar quantity of subgenomic RNA transcribed from ΔP1LucXN, which is identical to ΔP1LucCRE, but lacks any *cre* sequence (Fig. 1), resulted in no increase in luciferase activity beyond the minimal amount expressed at 3 h following transfection (Fig. 2A). In the presence of 2 mM guanidine, a potent inhibitor of HRV-14 RNA replication, neither ΔP1LucCRE nor ΔP1LucXN gave rise to an increase of luciferase activity beyond that present 3 h after transfection (Fig. 2A). Since there were no differences in luciferase activity between ΔP1LucCRE and ΔP1LucXN at 3 h following transfection in either the presence or absence of guanidine, this early low level of luciferase activity can be

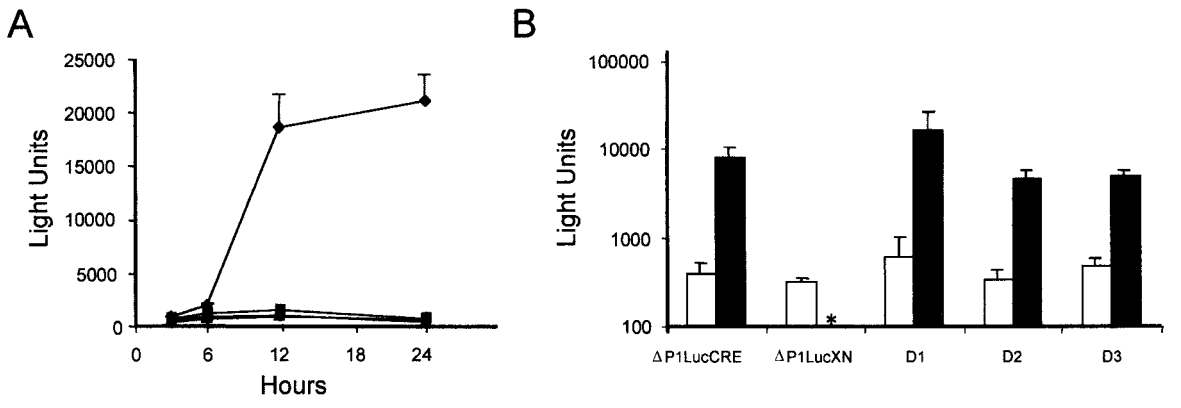

FIG. 2. (A) Luciferase activity derived from triplicate transfections of RNAs transcribed from plasmids pΔP1LucCRE and pΔP1LucXN. Transfected cells were processed and analyzed for luciferase activity at 3, 6, 12, and 24 h following transfection: ◆, ΔP1LucCRE in the absence of guanidine; ∗, ΔP1LucCRE in the presence of 2 mM guanidine, added immediately after transfection; and ΔP1LucXN in the absence (■) or presence (▲) of guanidine. (B) Luciferase activities expressed by ΔP1LucCRE, ΔP1LucXN, and the deletion mutants shown in Fig. 1, following RNA transfection of HeLa cells. At 3 h (open columns) and 24 h (solid columns) following transfection, cell lysates were harvested and assayed for luciferase activity. The results are the average of three independent transfections with error bars indicating the standard deviation. ∗, less than 100 light units.

considered to be due to the translation of the input RNAs in the absence of any RNA amplification. In contrast, the subsequent increase in luciferase activity between 3 and 24 h, which was observed only with ΔP1LucCRE and only in the absence of guanidine, reflects viral RNA replication. In support of this interpretation, the level of luciferase expression following expression of ΔP1LucCRE RNA was shown previously to closely follow its RNA replication kinetics as assessed by RNase protection assay (12).

As indicated above, previous studies by McKnight and Lemon mapped the *cre* to a 96-nt-long segment within the VP1 coding region of HRV-14 that is capable of forming a complex stem-loop structure within the positive-strand HRV-14 RNA (12) (Fig. 1). A mutational analysis confirmed the necessity for duplex formation within the apical stem of this structure. However, the requirement for the lower stem was less clearly documented, because only one of two mutant HRV-14 replicons with a 4-nt substitution in the lower stem was significantly impaired in replication (12). These data suggest that the lower duplex structure may not be essential for *cre* function. Thus, to better define the 5′ and 3′ boundaries of the minimal HRV-14 *cre*, we created a series of in-frame deletions within the previously identified 96-nt *cre* segment in the background of the replication-competent ΔP1LucCRE subgenomic replicon. As shown in Fig. 1, a series of double-deletion mutants were constructed (D1, D2, and D3), in which increasing lengths of sequences flanking the predicted apical stem-loop structure of the *cre* were removed from pΔP1LucCRE. In D1, the single-stranded regions 5′ and 3′ of the predicted complex stem-loop structure (nt 2318 to 2329 and 2405 to 2413) were deleted. In D2, the 5′ deletion was extended inward to include nt 2338 and the 3′ deletion to nt 2393, effectively removing most of the predicted distal duplex structure. In D3, the 5′ deletion was further extended to include nt 2353 and the 3′ deletion to nt 2387, removing the internal bulge-loops and leaving only a simple stem-loop structure with a 9-bp stem (Fig. 1).

RNA transcripts derived from pΔP1LucCRE and each of the three deletion mutants were electroporated into HeLa cells. Cell lysates were analyzed for luciferase activity at 3 h and 24 h following transfection, since, as shown above (Fig. 2A), an increase in luciferase expression during this period of time is indicative of RNA replication. Transfection of the three double-deletion mutants resulted in similar levels of luciferase expressed as a result of translation of the input RNA at 3 h after transfection (Fig. 2B). However, each also led to a significant increase in luciferase activity between 3 and 24 h following transfection (Fig. 2B), indicating that each RNA had undergone replication and that the minimal functional HRV-14 *cre* is located within the 33 nt remaining in mutant D3 (nt 2354 to 2386). In contrast, in cells transfected with ΔP1LucXN, which lacks any *cre* sequence (Fig. 1), luciferase activity decreased significantly between 3 and 24 h posttransfection (Fig. 2B), indicating a failure of viral RNA replication. These data indicate that the minimal functional HRV-14 *cre* is considerably smaller than the 96-nt structure proposed previously (12).

Nucleotide sequence required within the *cre* for RNA replication. Previous studies have indicated that extensive substitutions can be made within the duplex stem of the *cre* without compromising replication, provided that compensatory changes are introduced to maintain base pairing within the stem (12). Several nucleotide substitutions within the loop segment, however, were found to be lethal to replication. To better define the requirements for specific nucleotide sequence within the loop, we carried out an extensive mutational analysis of this region (nt 2363 to 2376). Using site-specific mutagenesis with degenerate oligonucleotide primers, we constructed a series of pΔP1LucCRE mutants containing single-base substitutions in which every possible nucleotide substitution was created at each of the nucleotide positions within the loop (Fig. 3A). (For convenience, we refer to these nucleotide positions according to their unique last two digits [e.g., "26" rather than "2326"]in Fig. 3 and the following sections.) Four of the intended substitutions, 63U, 66U, 70U, and 75U, introduced

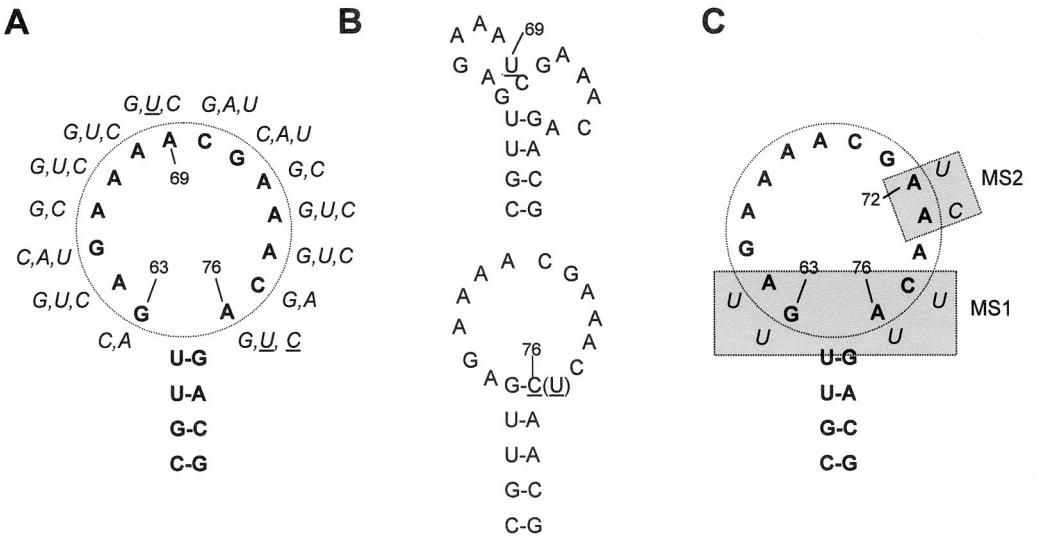

FIG. 3. Mutagenesis analysis of the loop of the HRV-14 *cre*. (A) Multiple single-nucleotide substitutions (shown in italic type outside of the circle) were created at each nucleotide between G63 and 76A in the loop of the *cre*. The underlined substitutions are those that were predicted by MFOLD to introduce changes in the secondary structure of the loop region. (B) MFOLD-predicted structures of the single nt 69U, 76C, or 76U mutants. The predicted structures of the 76C and 76U mutants were identical. (C) MS1 and MS2 are *cre* mutants with multiple nucleotide substitutions: MS1 contains 63U, 64U, 75U, and 76U substitutions; and MS2 contains 72U and 73C. In this and latter figures, the nucleotide position is indicated by the last two unique digits of the nucleotide map position (i.e., "63U" is nt 2363).

stop codons into the reading frame of ΔP1LucCRE, and hence could not be evaluated for their effect on replication as single-base substitutions. Thus, a total of 38 mutants were evaluated, each containing a point mutation at one of the 14 bases in the loop (Fig. 3A). These mutated *cre* sequences were analyzed by the MFOLD program to predict whether the single-nucleotide substitutions would lead to potential secondary structure alterations. Only three of them—69U, 76U, and 76C—were suggested by MFOLD to have a significant change in secondary structure from that of the wild-type *cre* (Fig. 3B).

Runoff transcripts representing the wild-type replicon and replicons with single-base substitutions within the *cre* were electroporated into HeLa cells. Replication was monitored by measuring luciferase activity at 3 and 24 h following electroporation. The efficiency of RNA replication was expressed as the fold increase in luciferase activity at 24 h over the luciferase activity at 3 h relative to that observed with the parental HRV-14 *cre* (ΔP1LucCRE), which was considered to be 100%. An increase in luciferase activity that was ≥15% of the parental level was considered indicative of significant RNA replication, while a fold increase in luciferase activity <15% that observed with the parent was considered to represent failure of significant replication and only the accumulation of translation products derived from input RNA. This 15% cutoff level represents approximately 3 standard deviations below the mean fold increase in luciferase expression observed between 3 and 24 h after transfection of the parental RNA, ΔP1LucCRE, in a series of four independent experiments, each done in triplicate (average fold increase, 32.9 ± 8.7). As shown in Fig. 4, most mutants replicated at levels either significantly above or below this breakpoint.

Surprisingly, at most positions within the loop (positions 64 to 66 and 70 to 75), any base substitution resulted in a replication-competent phenotype (Fig. 4). In contrast, any substitution of the three adenosines spanning positions 67 to 69, except for 69G, a purine transition, resulted in a failure to replicate, as evidenced by a lack of increase in the level of luciferase expression following electroporation of the RNA (Fig. 4). Since the 69U substitution causes a significant perturbation in the predicted secondary structure of the *cre* (Fig. 3B), it is not possible to discriminate whether the lethal effect of this mutation is related to an alteration in structure or primary sequence, or both. However the failure of 69C to replicate suggests the latter, since this substitution was not predicted to have altered the structure of the loop. These results indicate that A67, A68, and (to a lesser extent) A69 are essential for *cre* function in supporting RNA replication.

We created additional mutants to assess the effects of base substitutions that would result in the formation of stop codons within the *cre*. Since the 72U substitution creates a stop codon, we introduced another substitution at the second position of the codon, 73C. 73C by itself is replication competent, as was the multiple-substitution mutant MS2, which contains both 72U and 73C substitutions (Fig. 3C and 4). We could not use this approach to evaluate the effect of 66U, which creates a UAA stop codon, since any substitution at the relevant second base position, 67, was lethal (Fig. 4).

63U and 75U also introduce stop codons into the *cre* sequence. The further evaluation of these substitutions was complicated by the results of other substitutions at positions 63G and 76A, which are located at the junction of the stem and the loop in the predicted structure of the wild-type *cre* (Fig. 3A). Some substitutions at these bases, 63A and 76G, resulted in a replication-competent phenotype (Fig. 4). In contrast, other substitutions (63C, 76C, and 76U) were lethal or resulted in mutants with marginal replication capacity (Fig. 4). Although

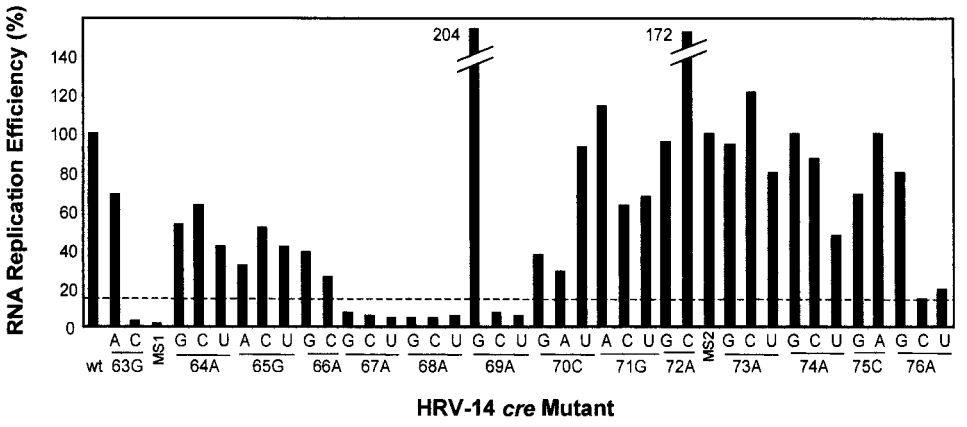

FIG. 4. Luciferase expression as a measure of replication of HRV-14 *cre* mutants in transfected HeLa cells. At 3 and 24 h following transfection, cell lysates were harvested and assayed for luciferase activity as described in Materials and Methods. Each column represents the fold increase in luciferase activity observed with a single RNA construct. The efficiency of RNA amplification was calculated as the ratio of luciferase expression at 24 h relative to luciferase expression at 3 h and compared with that observed with the parent ΔPLucCRE (set as 100%). The dashed line indicates a fold increase in luciferase activity equivalent to 15% of that observed with the parent RNA. Greater fold increases in luciferase activity were considered indicative of significant RNA amplification, while lesser increases were considered to be due primarily to translation from input RNA (see text). wt, wild type.

63G and 76A may form a noncanonical base pair in the wild-type structure (Fig. 3A), the two latter substitutions at position 76 have the potential to result in the formation of stronger base pair interactions at the base of the *cre* loop, 63G-76C or 63G-76U. Such base pairing could reduce the size of the loop from 14 nt to 12 nt or otherwise change its conformation (Fig. 3B). Thus, we suspected that the inhibition of replication by the 76C and 76U substitutions might be caused by alteration in the secondary or tertiary structure of the loop. To test this hypothesis, and at the same time to evaluate the effect of the remaining two substitutions that result in stop codons, 63U and 75U, we created the multiple-substitution mutant MS1 shown in Fig. 3C. This mutant contains 63U, 64U, 75U, and 76U substitutions and is both free of stop codons and not capable of base pairing between positions 63 and 76. Although the 4 base substitutions in MS1 do not change the predicted secondary structure, this mutated *cre* failed to support RNA replication (Fig. 4). Thus, it is not clear whether the negative effects of some single-nucleotide substitutions at positions 63 and 76 result from alterations of the secondary structure alteration, rather than changes in the primary sequence of the RNA (see Discussion). Similar to the situation at position 69A, it seems that only a purine transition is well tolerated at positions 63G and 76A.

In summary, no substitution of 67A or 68A was permissible. At the position immediately following these two adenosines, 69A, only a purine transition was acceptable. This was also the case with the 2 nt at the bottom of the loop, 63G and 76A, at which only purine transitions were tolerated. In contrast, any substitution was permitted at other positions in the loop without significantly impairing the *cre* function in replication. These conclusions are summarized in Fig. 5.

Capacity of mutant *cre* RNAs to support VPg uridylylation in vitro. The HRV-14 *cre* has been shown to be an effective template for the uridylylation of the VPg proteins of either HRV-14 or PV-1 type 1 by the PV-1 $3D^{pol}$ enzyme (17). This prompted us to investigate whether the capacity of the *cre* mutants to support replication in vivo would correlate with their ability to function in an in vitro VPg uridylylation reaction. VPg uridylylation reactions were carried out with synthetic PV-1 VPg, and recombinant PV-1 $3D^{pol}$ and $3CD^{pro}$, as described previously (17). RNA transcripts representing each of the HRV-14 *cre* mutants were added to individual reaction mixtures. The efficiency of the reaction was measured by PhosphorImager quantification of the yield of uridylylated VPg, VPg-pU, and VPg-pUpU, as shown in Fig. 6. In each experiment, the efficiency of uridylylation was compared to that of a reaction mixture containing the wild-type HRV-14 *cre* RNA.

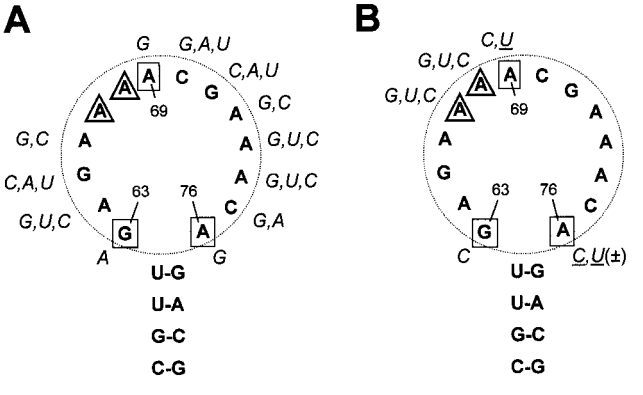

FIG. 5. Summary of the effect of nucleotide substitutions within the HRV-14 *cre* loop on RNA replication. Only the loop and the proximal 4 bp within the stem are shown in this figure. (A) Replication-competent HRV-14 *cre* mutants. (B) Mutations with a lethal effect on HRV-14 replication that represent those contributing critically to *cre* function (see legend to Fig. 4). Underlined substitutions are those predicted by MFOLD to introduce changes in the secondary structure of the RNA. The nucleotides in triangles are those for which no substitution was permissible, while the nucleotides in the squares are those for which some substitutions were permissible. At the other loop positions, any nucleotide substitution was permissible, provided that it did not introduce a stop codon.

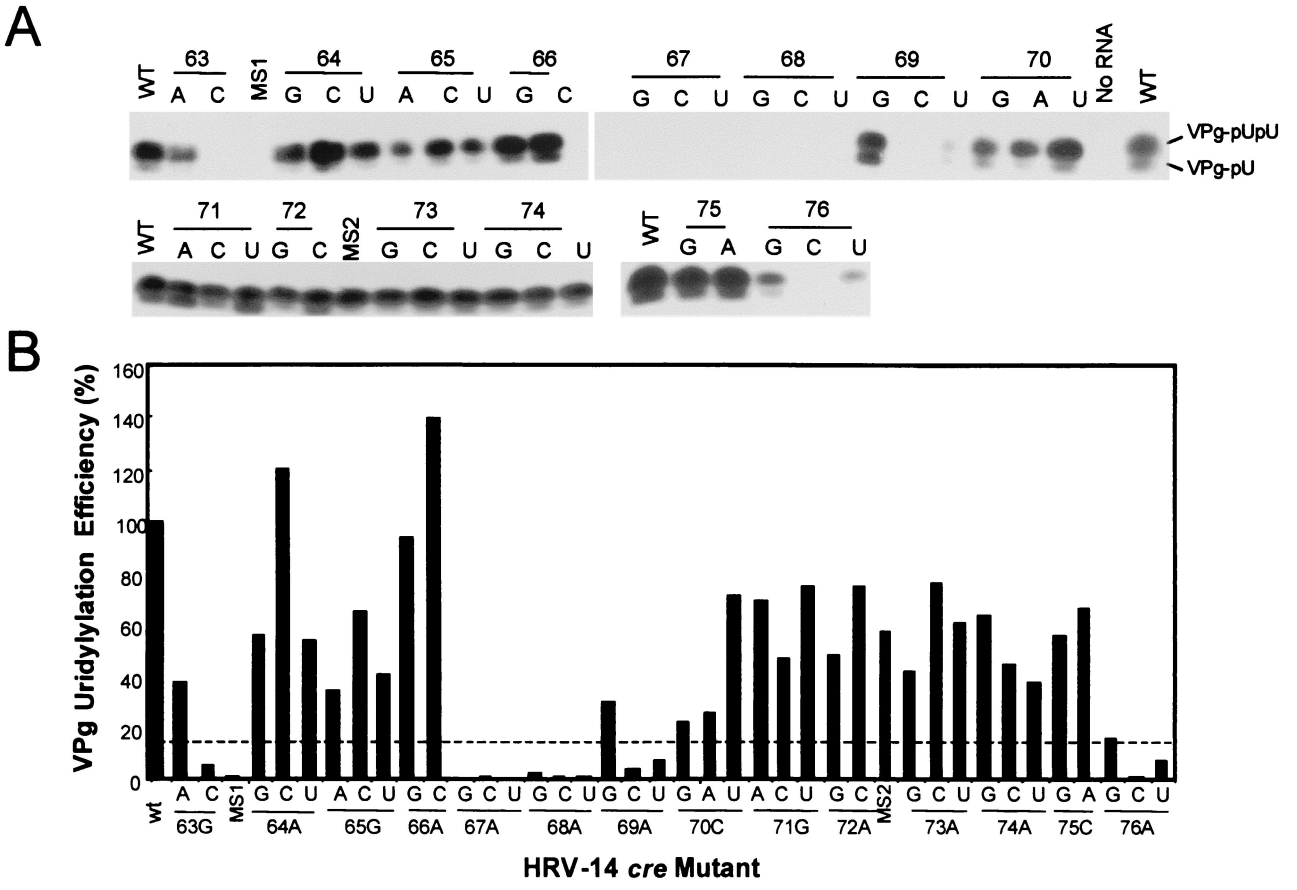

FIG. 6. Capacity of mutated HRV-14 *cre* RNA transcripts to support in vitro VPg uridylylation. (A) The products of in vitro VPg uridylylation reactions were separated on Tricine-SDS-PAGE gels (13.5% polyacrylamide) and visualized by autoradiography. WT, wild type (ΔPLucCRE). (B) Quantitation of VPg uridylylation reaction products by PhosphorImager. Each column represents the relative abundance of uridylylated VPg relative to the amount produced in control reactions containing the parental *cre* RNA (set at 100%). The dashed line indicates 15% of the amount of product produced with the parent RNA.

As shown in Fig. 6A, the PV-1 $3D^{pol}$ enzyme efficiently directed the uridylylation of the PV-1 VPg protein in the presence of the wild-type HRV-14 *cre* RNA. Those mutant *cre* sequences that retained the ability to support RNA replication also remained active in the VPg uridylylation reaction, although with various levels of efficiency producing various amounts of VPg-pU and VPg-pUpU. A few mutants produced yields of uridylylated VPg that were comparable to or higher than that produced with the wild-type *cre*, such as 64C, 66C, or 66G (Fig. 6A). However, most of the mutant *cre* RNAs produced lower yields of the uridylylated protein (15 to 80% of the wild-type level), such as 63A, 64G, 64U, 69G, 76G, and all substitutions at positions 65 and 70 to 75 (Fig. 6).

As shown previously, each of the nucleotide substitutions at positions 67 and 68 abolished replicon amplification (Fig. 4). Importantly, these substitutions also failed to produce detectable uridylylation products (Fig. 6). The 63C, 69C, and 76C substitutions, as well as the multiple mutant MS1, each of which was also deficient in RNA replication (Fig. 4), resulted in yields of uridylylated VPg that were no more than the background level (Fig. 6). The marginally replicating mutant 76U and a nonreplicating mutant 69U (Fig. 4) produced yields of uridylylated VPg that were less than 10% of the wild-type level. There was thus a good correlation between the capacity of each mutant *cre* to support RNA replication and its ability to function in the in vitro uridylylation reaction, as shown schematically in Fig. 7.

DISCUSSION

To date, *cre*s have been identified within the protein-coding sequences of viruses representing three genera of picornaviruses: rhinoviruses, enteroviruses, and cardioviruses (4, 5, 9, 11, 12). These *cre*s are similar in that they are all located within protein-coding sequence, but function at the level of RNA. Each is predicted to form a stem-loop structure about 30 to 65 nt in length, generally involving nucleotide tracts with low P-num values supporting the likelihood that the structure is conserved and thus biologically significant (16). The available evidence suggests that these RNA structures are required within the positive strand of the RNA for efficient initiation of minus-strand RNA synthesis (12) and that they are likely to be common to the RNA replication scheme of most if not all picornaviruses.

However, there are differences in these *cre*s that are also remarkable. First, they are located in different regions (VP1,

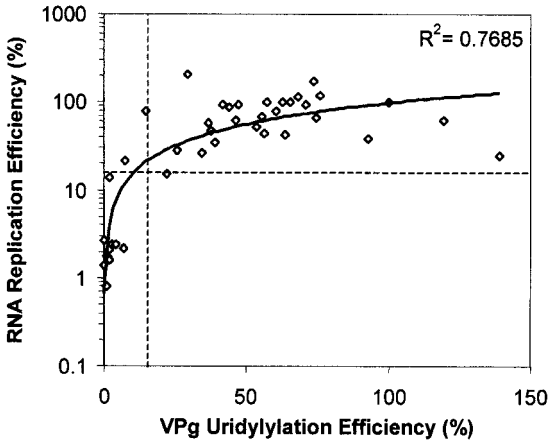

FIG. 7. Least-squares-fit plot showing the correlation between the efficiencies of each mutant *cre* to support in vitro VPg uridylylation and to function in RNA replication, based on the data presented in Fig. 4 and 6. The dotted lines represent values for replication capacity and uridylylation activity equal to 15% of the wild-type *cre*. The R^2 value obtained in a transformed regression model was 0.7685.

VP2, 2A, or 2C coding region) of the genome, suggesting that *cre* function is not dependent on a specific location and that different viruses have evolved *cre*s at different sites within the genome in ways conducive to their dual roles as both replication element and protein-coding sequence. Another surprising difference, considering their common roles in RNA replication, is the extent of the diversity that is evident in their primary sequences as well as predicted secondary structures. The sequence differences present in the HRV-14, PV-1, and HRV-2 *cre*s (Fig. 8A) are even more surprising, since the HRV-14 *cre* is capable of substituting for the PV-1 and HRV-2 *cre*s in VPg uridylylation reactions with PV-1 and HRV-2 enzymes (4, 17). This suggests that the PV-1 and rhinovirus enzymes involved recognize some common sequence and/or structural features in these *cre*s. Our primary aim in this study was to identify the sequences that are critical for HRV-14 *cre* function and, by comparing these with other known or predicted *cres*, to identify those sequences and structural features that are important for RNA replication.

Since previous results suggested that the minimal functional HRV-14 *cre* (12) was significantly larger (96 nt) than the *cre*s identified subsequently in other picornaviruses (4, 5), we created a series of deletion mutants in which the sequences flanking the apical loop of the structure predicted for the HRV-14 *cre* were progressively deleted (Fig. 1). The ability of each of these mutants to support the replication of HRV-14 RNA (Fig. 2B) indicated that the minimal functional *cre* resides within a 33-nt sequence that is predicted to form a simple stem-loop (nt 2354 to 2386) (Fig. 1). The HRV-14 *cre* is thus no larger than the *cre* identified in other picornaviruses.

These results indicate that only the top stem and loop se-

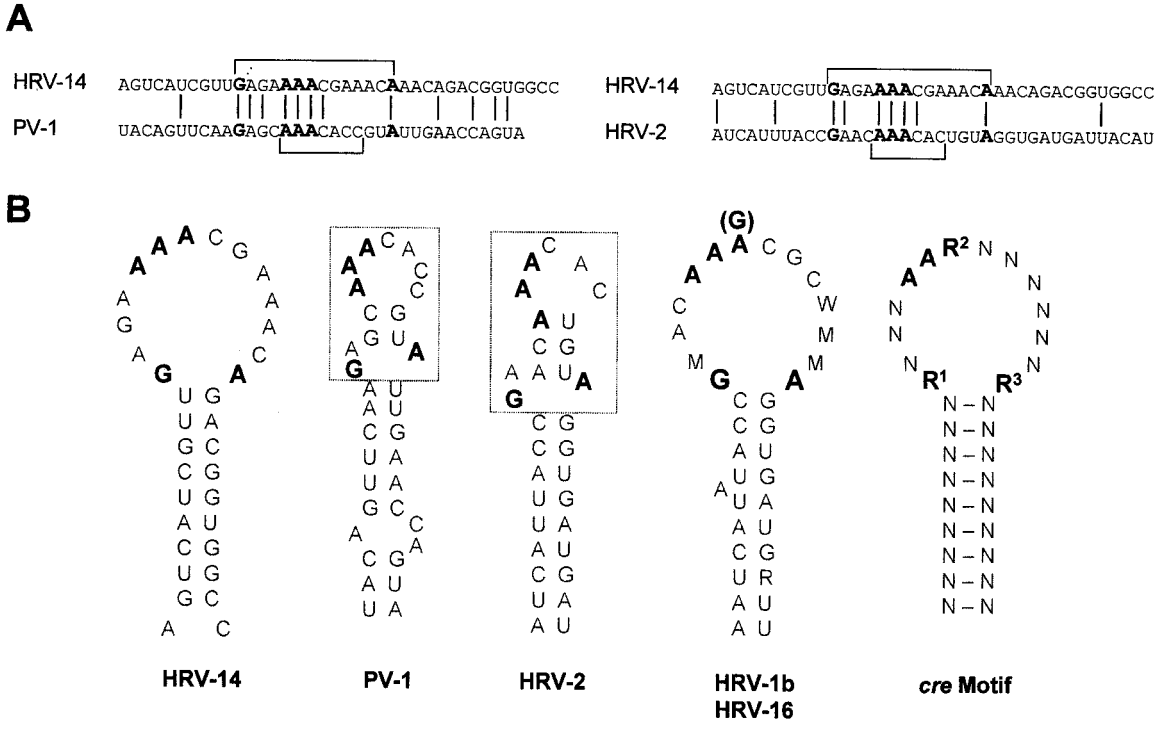

FIG. 8. Comparison of the sequences and predicted structures of the *cre*s of human rhinoviruses and enteroviruses. (A) Alignments of the sequence of the HRV-14 *cre* with the PV-1-type 1 *cre* sequence (left) and the HRV-2 *cre* sequence (right). The brackets depict the nucleotide segments predicted by MFOLD to form the terminal loops of the *cre* hairpins. (B) MFOLD predictions of the structures of the *cre*s of HRV-14, PV-1 (5), HRV-2 (4), and the predicted *cre*s of HRV-1b and -16 (4). The conserved critical bases identified by mutational analysis of the HRV-14 *cre* are shown in boldface. The proposed equivalent structures in the PV-1 and HRV-2 *cre*s are enclosed in dashed boxes. At the far right is shown the proposed common structure for HRV and enterovirus *cre*s. R = A/G; W = A/U; M = A/C; N = any nucleotide.

quences of the originally described 96-nt *cre* structure (12) are required for replication of HRV-14 RNA and that the large internal loop and lower duplex stem (see ΔP1LucCRE structure in Fig. 1) are not essential. Despite this, McKnight and Lemon (12) found that some mutations in the lower stem were lethal to replication of HRV-14 RNA. Since the sequences forming the lower stem are located outside of the region, we have shown here to contain the minimal functional *cre* (Fig. 1), these results are best explained by changes in the folded structure of the top loop and stem of the *cre* mediated by mutations in the lower stem. If this interpretation is correct, the tertiary structure of the *cre* loop is critically important to its ability to function in RNA replication and probably also uridylylation of VPg. In general, however, it appears that a stem of 8 to 10 bp, similar to what we have determined for the minimal HRV-14 *cre*, is sufficient to support *cre* function. Disruption of the lower part of the PV-1 *cre* stem (leaving 9 bp at the base of the loop) had little effect on *cre* function (24). In addition, the predicted cardiovirus *cre* structures have stems formed by 8 to 10 bp (9).

We also carried out an extensive mutational analysis of the loop of the HRV-14 *cre*, because previous work points to its importance in RNA replication (12). The HRV-14 *cre* presents a unique opportunity for such a mutational analysis, since unlike the PV-1 or HRV-2 *cre*, it is located within the P1 region that encodes capsid proteins that are not necessary for RNA replication (12). Thus, mutations in the HRV-14 *cre* do not alter the amino acid sequence of proteins that contribute to the replicase. This distinguishes the *cre* mutants we have studied here from many of the mutations that have been studied previously in the PV-1 or HRV-2 *cre*s (4, 17) and has also allowed us to do a more complete analysis. The fact that we found a strong correlation between the effects of these HRV-14 mutations on VPg uridylylation in vitro and on RNA replication in vivo (Fig. 7) provides additional indirect, but nonetheless strong, evidence that the ability of the *cre* to function as a template for VPg uridylylation is essential for viral RNA synthesis.

We found that an AAA triplet (nt 2367 to 2369, or 67A, 68A, and 69A) located in the 5′ half of the loop and 2 nt, 63G and 76A, at the bottom of the loop, are important for *cre* function, while there are no requirements for specific bases at other positions (Fig. 5). Any substitution within the AAA triplet abrogated RNA replication, except for the substitution of 69A with 69G. These results are reminiscent of previous studies of the PV-1 *cre*, in which the mutation of either of the first two A's of the AAA triplet within the 5′ half of the loop in the PV-1 element abolished infectivity (24). Mutation of these adenosines in the HRV-2 *cre* also abrogated uridylylation of VPg and replication of the virus (4). This AAA triplet is part of the AAACA motif identified by Rieder et al. (24) in the PV-1 *cre* loop and considered to be a common feature of the *cre*. The mutational analysis of the HRV-14 *cre* shown in Fig. 4 and 6, however, demonstrates that the CA dinucleotide within the AAACA motif is not necessary for replication or uridylylation. We also found that 63G and 76A, located at the junction of the *cre* loop and stem, were critically important for *cre* activity. As with 69A, only purine transition mutations were permissible at these bases.

Alignments of the sequences around the AAA triplet in the HRV-14, PV-1, and HRV-2 *cre*s indicate that the critical base residues we have identified in the HRV-14 *cre* are perfectly conserved in these other *cre*s (Fig. 8A, boldface type). This includes the 63G and 76A bases at the junction of the HRV-14 *cre* loop and stem. However, in contrast to the HRV-14 loop sequence, which is predicted by MFOLD to be 14 nt in length, the homologous sequences in the PV-1 and HRV-2 *cre*s are predicted to contain several base pairs and an internal loop and to fold differently from HRV-14 as well as each other (Fig. 8B). These structure predictions have not been tested by any physical means, however, nor by appropriate mutational analyses, so their validity is unknown. Despite the differences in the computer-predicted secondary structures, we suspect that these sequences are similarly structured in all three *cre*s. Such structural homology would make the observation that these *cre*s are functionally exchangeable with each other in uridylylation reactions understandable (4, 17). Alternatively, it is possible that the binding of proteins such as 3CD, 3D, and VPg to the PV-1 and HRV-2 elements in the earliest steps of the uridylylation reaction might cause a change in the conformation of the RNA, opening up internal base pairs so that the PV-1 and HRV-2 structures resemble that of the HRV-14 *cre*.

Gerber et al. (4) identified potential *cre*s in two rhinoviruses that are closely related to HRV-2, HRV-16 and HRV-1b. These proposed *cre* sequences were located at essentially the same position in the genome as the HRV-2 *cre*. Again, the bases that we found to be essential for HRV-14 *cre* activity are conserved in these putative *cre*s, including 63G and 76A at the junction of the loop and the stem. It is interesting to note, however, that in the proposed HRV-16 *cre*, the AAA triplet is replaced with AAG. We found this substitution to be functional in the HRV-14 background, both for replication and for uridylylation (Fig. 4 and 6).

Based on our mutational analysis of the HRV-14 *cre* and comparisons of the HRV-14 *cre* sequence with the *cre*s of other viruses, we propose a common motif for the loop segment of rhinovirus and enterovirus *cre*s that likely defines a common structure (Fig. 8B): $R^1NNNAAR^2NNNNNNR^3$.

We predict that an AAR triplet will be present in the 5′ half of the loop sequence in all these replication elements. At the third base position of this triplet (R^2), the base may be either A or G, but there is clearly a preference for A. This is also the case for R^3, while a G is preferable at R^1. R^1 and R^3 are located at the extreme ends of the loop and seem likely to be involved in a non-Watson-Crick base pair interaction (see below). At the remaining positions, A, C, G, or U appears to be equivalently acceptable for both replication and uridylylation, and the specific base present is likely to be determined more by the requirement for coding specific amino acids than by a requirement for preservation of *cre* function. However, a mutation involving the substitution of 4 contiguous bases within the loop sequence (69A through 72A) was found previously by McKnight and Lemon (12) to be lethal for replication, even though we have shown here that each of the individual base substitutions in this mutant was permissive for replication and uridylylation. It is likely that the failure of the multiple-substitution mutant to function as a *cre* was due to perturbation of the structure of the loop following substitution of such a large proportion of the bases within it.

All of the known cardiovirus *cre* sequences also possess an AAA motif that is predicted to be at least partially single

stranded in these viruses. A mutation at the second A of this motif in the Theiler's virus *cre* was shown to be lethal for RNA replication (9). However, the cardiovirus *cre* appears to have a very different structure from that of the PV-1 or rhinovirus *cre*, because the homologous AAA triplet in Theiler's virus appears to be located within a small bulge-loop that is part of a larger hairpin structure (9). This difference in structure is consistent with the failure of the HRV-14 *cre* to substitute for the cardioviral *cre* in supporting viral replication (9), as well as the greater phylogenetic distance between the cardioviruses and these other picornaviral genera.

Studies by Paul et al. (17) and Gerber et al. (4) have shown that the PV-1 *cre* acts as the primary template for VPg uridylylation in vitro, a reaction that requires only synthetic VPg, UTP, purified PV-1 RNA, PV-1 RNA polymerase $3D^{pol}$, and Mg^{2+}. Mutations that abolish the ability of the PV-1 or HRV-2 *cre* to act as template for VPg uridylylation in vitro also eliminate their ability to support viral RNA replication in vivo (4, 17). Substitution of the AAA triplet in the HRV-2 *cre* with CAA also led to a change in the specificity of the nucleotidylylation reaction, with the covalent addition of guanine to VPg leading to VPg-pG (4). These observations suggest that the AAA triplet functions as a template for the nucleotidylylation of VPg by using a slide-back mechanism in which the most 5′ adenosine of the AAA triplet templates the nucleotide to be linked to VPg. This indicates that the conserved AAR^2 residues within the loop of the rhinovirus and enterovirus *cre*s are likely to be located on the surface of the folded RNA structure. The conserved 63G and 76A residues (Fig. 8B) have the potential to form a non-Watson-Crick closing pair at the base of the loop. Recent studies of synthetic RNA aptomers suggest that the presence of a GA closing pair significantly influences the structure of the adjacent RNA loop and may have a critical role in determining the ability of the loop to form stable loop-loop interactions (2). While there is no evidence that the *cre* loop is involved in a loop-loop interaction, we speculate that the conserved 63G and 76A residues form such a closing pair and that the presence of this closing pair contributes in an important way to the structure of the *cre* loop that is required for proper presentation of the AAR^2 triplet as the template for uridylylation.

ACKNOWLEDGMENTS

This work was supported by grants from the National Institute of Allergy and Infectious Diseases (RO1-AI140282) (S.M.L.) and the McLaughlin Endowment of the University of Texas Medical Branch (Y.Y.).

REFERENCES

1. **Andino, R., G. E. Rieckhof, P. L. Achacoso, and D. Baltimore.** 1993. PV-1 RNA synthesis utilizes an RNP complex formed around the 5′-end of viral RNA. EMBO J. **12:**3587–3598.
2. **Duconge, F., C. Di Primo, and J. J. Toulme.** 2000. Is a closing "GA pair" a rule for stable loop-loop RNA complexes? J. Biol. Chem. **275:**21287–21294.
3. **Flanegan, J. B., R. F. Petterson, V. Ambros, N. J. Hewlett, and D. Baltimore.** 1977. Covalent linkage of a protein to a defined nucleotide sequence at the 5′-terminus of virion and replicative intermediate RNAs of PV-1. Proc. Natl. Acad. Sci. USA **74:**961–965.
4. **Gerber, K., E. Wimmer, and A. V. Paul.** 2001. Biochemical and genetic studies of the initiation of human rhinovirus 2 RNA replication: identification of a *cis*-replicating element in the coding sequence of $2A^{pro}$. J. Virol. **75:**10979–10990.
5. **Goodfellow, I., Y. Chaudhry, A. Richardson, J. Meredith, J. W. Almond, W. Barclay, and D. J. Evans.** 2000. Identification of a *cis*-acting replication element within the poliovirus coding region. J. Virol. **74:**4590–4600.
6. **Jang, S. K., H.-G. Krausslich, M. J. H. Nicklin, G. M. Duke, A.C. Palmenberg, and E. Wimmer.** 1988. A segment of the 5′ nontranslated region of encephalomyocarditis virus RNA directs internal entry of ribosomes during in vitro translation. J. Virol. **62:**2636–2643.
7. **Lee, W.-M., S. S. Monroe, and R. R. Rueckert.** 1993. Role of maturation cleavage in infectivity of picornaviruses: activation of an infectosome. J. Virol. **67:**2110–2122.
8. **Lee, Y. F., A. Nomoto, B. M. Detjen, and E. Wimmer.** 1977. A protein covalently linked to poliovirus genome RNA. Proc. Natl. Acad. Sci. USA **74:**59–63.
9. **Lobert, P.E., N. Escriou, J. Ruelle, and T. Michiels.** 1999. A coding RNA sequence acts as a replication signal in cardioviruses. Proc. Natl. Acad. Sci. USA **96:**11560–11565.
10. **Lyle, J. M., A. Clewell, K. Richmond, O. C. Richards, D. A. Hope, S. C. Schultz, and K. Kirkegaard.** 2002. Similar structural basis for membrane localization and protein priming by an RNA-dependent RNA polymerase. J. Biol. Chem. **277:**16324–16331.
11. **McKnight, K. L., and S. M. Lemon.** 1996. Capsid coding sequence is required for efficient replication of human rhinovirus 14 RNA. J. Virol. **70:**1941–1952.
12. **McKnight, K. L., and S.M. Lemon.** 1998. The rhinovirus type 14 genome contains an internally located RNA structure that is required for viral replication. RNA **4:**1569–1584.
13. **Melchers, W. J. G., J. G. J. Hoenderop, H. J. B. Slot, C. W. A. Pleij, E. V. Pilipenko, V. I. Agol, and J. M. D. Galama.** 1997. Kissing of the two predominant hairpin loops in the coxsackie B virus 3′ untranslated region is the essential structural feature of the origin of replication required for negative-strand RNA synthesis. J. Virol. **71:**686–696.
14. **Mirmomeni, M. H., P. J. Hughes, and G. Stanway.** 1997. An RNA tertiary structure in the 3′ untranslated region of enteroviruses is necessary for efficient replication. J. Virol. **71:**2363–2370.
15. **Palmenberg, A. C.** 1990. Proteolytic processing of picornaviral polyprotein. Annu. Rev. Microbiol. **44:**603–623.
16. **Palmenberg, A. C., and J.-Y. Sgro.** 1997. Topological organization of picornaviral genomes: statistical prediction of RNA structural signals. Semin. Virol. **8:**231–241.
17. **Paul, A. V., E. Rieder, D. W. Kim, J. H. Van Boom, and E. Wimmer.** 2000. Identification of an RNA hairpin in poliovirus RNA that serves as the primary template in the in vitro uridylylation of VPg. J. Virol. **74:**10359–10370.
18. **Paul, A. V., J. H. Van Boom, D. Filippov, and E. Wimmer.** 1998. Protein-primed RNA synthesis by purified PV-1 RNA polymerase. Nature **393:**280–284.
19. **Pelletier, J., and N. Sonenberg.** 1988. Internal initiation of translation of eukaryotic mRNA directed by a sequence derived from PV-1 RNA. Nature **334:**320–325.
20. **Pilipenko, E. V., S. V. Maslova, A. N. Sinyakov, and V. I. Agol.** 1992. Towards identification of *cis*-acting elements involved in the replication of enterovirus and rhinovirus RNAs: a proposal for the existence of tRNA-like terminal structures. Nucleic Acids Res. **20:**1739–1745.
21. **Pilipenko, E. V., V. Poperechny, S. V. Maslova, W. J. G. Melchers, H. J. Bruins Slot, and V. I. Agol.** 1996. Cis-element, oriR, involved in the initiation of (−) strand PV-1 RNA: a quasi-globular multi-domain RNA structure maintained by tertiary ('kissing') interactions. EMBO J. **15:**5428–5436.
22. **Racaniello, V. R., and D. Baltimore.** 1981. Cloned PV-1 complementary DNA is infectious in mammalian cells. Science **214:**916–919.
23. **Regenmortel, M. H. V., C. M. Fauquet, D. L. Bishop, E. B. Carstens, M. K. Estes, S. M. Lemon, J. Maniloff, M. A. Mayo, D. J. McGeogh, R. B. Pringle, and R. B. Wickner.** 2000. Virus taxonomy: the classification and nomenclature of viruses. The Seventh Report of the International Committee on Taxonomy of Viruses. Academic Press, San Diego, Calif.
24. **Rieder, E., A. V. Paul, D.W. Kim, J. H. Van Boom, and E. Wimmer.** 2000. Genetic and biochemical studies of poliovirus *cis*-acting replication element *cre* in relation to VPg uridylylation. J. Virol. **74:**10371–10380.
25. **Rohll, J. B., D. H. Moon, D. J. Evans, and J. W. Almond.** 1995. The 3′ untranslated region of picornavirus RNA: features required for efficient genome replication. J. Virol. **69:**7835–7844.
26. **Rueckert, R. R., and E. Wimmer.** 1984. Systematic nomenclature of picornavirus proteins. J. Virol. **50:**957–959.
27. **Todd, S., J. H. C. Nguyen, and B. L. Semler.** 1995. RNA-protein interactions directed by the 3′ end of human rhinovirus genomic RNA. J. Virol. **69:**3605–3614.
28. **Wimmer, E., C. U. T. Hellen, and X. Cao.** 1993. Genetics of PV-1. Annu. Rev. Genet. **27:**353–436.